European Journal of Pharmaceutical Sciences 170 (2022) 106096

Contents lists available at ScienceDirect

European Journal of Pharmaceutical Sciences

journal homepage: www.elsevier.com/locate/ejps

Enhancement of skin permeation of fluorescein isothiocyanate-dextran 4 kDa (FD4) and insulin by thermalporation

Naoto Ono [a], Tomoya Iibuchi [a], Hiroaki Todo [a,*], Shoko Itakura [a], Hirotoshi Adachi [b], Kenji Sugibayashi [a]

[a] Faculty of Pharmacy and Pharmaceutical Sciences, Josai University, 1-1 Keyakidai, Sakado, Saitama 350-0295, Japan
[b] PassPort Technologies, Inc., 5580 Morehouse Drive, Suite 120, San Diego, CA 92121, USA

A B S T R A C T

Thermalporation has gained attention as a physical means to enhance skin permeation by creating micropores in the primary skin barrier, stratum corneum, which allows much higher permeation of middle and high molecular weight biopharmaceuticals. In the present study, a PassPort® system (PS) was used as a thermalporation device, and the obtained change in permeation resistance of drugs was evaluated using a parallel skin permeation-resistance model. In addition, the blood concentration–time profile after topical application of insulin was also investigated with the PS treatment.

Fluorescein isothiocyanate-dextran (FD-4) and insulin were used as model middle molecular weight drugs. Micropores created by the PS treatment were measured using an optical microscope. An *in vitro* skin permeation and an *in vivo* pharmacokinetics experiments were done with FD-4 and insulin, respectively. Barrier function recovery after the PS treatment was evaluated with changes in the electrical skin resistance.

About 960-fold higher skin permeation of FD-4 was observed by PSs treatment (4 milliseconds (ms), 200 micropores/cm^2). A gradually increased blood concentration of insulin was observed by the PSs treatment, and the relative bioavailability of insulin was 21.1% compared with subcutaneous injection. Skin resistance value was dramatically decreased immediately after the PS treatment, but its value was turned into the initial one by 12 h.

The thermalporation is effective for improving skin permeation of FD-4 and transdermal absorption of insulin. These results suggested that the PS treatment may be utilized to increase the skin permeation of topically applied FD-4 and insulin.

Introduction

Nowadays, middle-size biomolecules such as peptides and nucleic acids with various biological activities can be chemically synthetized (Nagamune, 2017). They are usually administered to patients via intravenous or subcutaneous routes due to their low permeability through the intestinal membrane.

Skin is the most accessible drug administration site on the human body. Physical devices such as needle-free injectors and hollow microneedles have become available to administer drugs (Waghule et al., 2019; Hogan et al., 2015; Prausnitz et al., 2004). These devices enable reliable drug administration with a high reproducibility and have strong advantages for the administration of middle and high molecular weight biomedical compounds such as nucleic acids, peptides, vaccines, and antibodies (Zhao et al., 2006; Sulaiman et al., 2019).

Thermal ablation techniques can improve the skin permeation of drugs by chemical heating (Wood et al., 2011), element-based heating (Badkar et al., 2007, 2003), radiofrequency, and laser irradiation. Chemical heating-based techniques with iron oxide (controlled heat-assisted drug delivery [CHADD^{TM}]) significantly improved the skin permeation of lidocaine and prilocaine (Sawyer et al., 2009). Element-based heating, so called thermalporation, with PassPort® system (PS) increased the skin permeation of calcein (M.W. 622 Da) by 760-fold (Park et al., 2008), and radiofrequency-based thermal ablation enhanced skin permeation increased that of diclofenac sodium and granisetron HCl by 8-fold and 30-fold, respectively, compared with their passive diffusion (Sintov et al., 2003). Thermal ablation generates micropores by selective vaporization of the stratum corneum (SC) by applying heat. This technique may not require sterilization processes, unlike with the use of microneedles. Skin permeation was increased by skin ablation by depletion or removal of the SC; however, the permeation enhancement effect may depend on the physicochemical properties of drugs, type of application device, and its application conditions. Understanding changes in barrier function of the SC by skin ablation may lead to the development of devices to achieve a high level of skin permeation.

PS was used as a thermal ablation device in the present study because it performs suction to contact the filaments to the skin firmly and applies

* Corresponding author at: Faculty of Pharmacy and Pharmaceutical Sciences, Josai University, 1-1 Keyakidai, Sakado, Saitama 350-0295, Japan.
E-mail address: ht-todo@josai.ac.jp (H. Todo).

https://doi.org/10.1016/j.ejps.2021.106096
Received 10 August 2021; Received in revised form 18 November 2021; Accepted 9 December 2021
Available online 17 December 2021

controlled thermal energy to the outer layer of skin briefly (e.g. several milliseconds) to physically create permeation routes for drugs, so this technique can provide reliable drug administration with high reproducibility.

Many reports have been published on the skin permeation enhancement of middle or high molecular weight biomolecules by physical means, such as microneedles, electroporation, iontophoresis, and thermal ablation with *in vitro* and *in vivo* experiments (Prausnitz, 2008; Wu et al., 2006). Badkar et al. (2007) have reported that enhancement of skin permeation of interferon alpha-2b was obtained by application of thermalporation. In addition, application conditions (temperature–time profile and geometry of the filament) related to the size of micropores created may be related to the enhancement effect. However, even though a skin permeation enhancement effect was observed with certain drugs by physical means, it is difficult to develop an application device without theoretically understanding the enhancement mechanism and estimation of the bioavailability of topically applied drugs. In the present study, pig skin, was used an alternative to human skin in the *in vitro* experiments to reveal changes in drug permeation resistance and to clarify the enhancement effect on the skin permeation of fluorescein isothiocyanate-dextran (*M.W.* av. 4,000, FD-4) by PS treatment. In addition, insulin (*M.W.* 5808), a model middle size molecular weight drug, was selected to investigate the blood concentration–time profile obtained after PS treatment in rats.

2. Materials and method

2.1. Materials

PS, a thermalporation device, was provided by PassPort Technologies, Inc. (San Diego, CA, USA). Three PS devices with different pulse periods of thermal energy were used in the present study. The devices with the shortest application period (1.1 ms), longest application period (4 ms), and an intermediate application period (2 ms) were named $PS_{1.1ms}$, PS_{2ms}, and PS_{4ms}, respectively.

Fluorescein isothiocyanate dextran (M.W., 4000, FD-4), methylene blue, and Glucose CII-Test Wako Kits were purchased from FUJIFILM Wako Pure Chemical Co., Ltd. (Osaka, Japan). Human insulin (Humulin R U-100) was purchased from Eli Lilly Japan (Kobe, Japan). All reagents were of analytical grade and were used as received without further purification.

2.2. Animals

WBN/ILA-Ht male hairless rats (body weight 200–250 g, 8 weeks old) were purchased from Ishikawa Experimental Animals (Saitama, Japan). Male Wistar rats (weight 180–200 g, 8 weeks old) were purchased from Sankyo Labo Service Corporation, Inc. (Tokyo, Japan). Hairless rats and Wistar rats were kept in a room regulated at 25 ± 2°C with a light/dark cycle (on and off time: 9:00–21:00) every 12 h. Water and food (MF, Oriental Yeast Industry, Tokyo, Japan) were freely available. Animal care and experiments were conducted in accordance with the Josai University Experimental Animal Regulations after obtaining the consent from the Josai University Animal Experiment Management Committee (JU19007).

2.3. Application of PS to skin

A re-usable thermal ablation PS device consisted of a handheld applicator and a porator. The porator in PS involves 200 resistive stainless filaments distributed within $1cm^2$ and connected with thick conductive copper traces/paths (Fig. 1). Filament are simultaneously heated for designated periods (1.1 ms, 2 ms, or 4 ms), and achieve 600°C to 700°C. Initially, the applicator equipped with the porator was placed over the skin surface. The skin was adhered to the porator using suction force, the porator in the loaded applicator then applied thermal energy by passing electrical energy to the filaments for microseconds, which was activated by pressing a button.

2.4. In vitro skin permeation experiment

Yucatan micropig (YMP) dorsal skin was purchased from Japan Charles River Corporation (Yokohama, Japan) and stored frozen at -80°C before the *in vitro* skin permeation experiment. Frozen YMP skin was thawed in warm water at 32°C. After thawing, the skin surface of the YMP was carefully washed with purified water to avoid damaging the SC. Then, the skin was split using a dermatome (Acculan 3Ti Dermatome; Aesculap-a B. Braun Company, Melsungen, Hessen, Germany) to adjust the thickness to 550 μm from the skin surface. The thickness of the dermatomed skin was confirmed using a thickness gauge (SM-112, Teclock Co. Ltd., Okaya, Nagano, Japan). The dermatomed skin was mounted in a vertical diffusion cell (effective transmission area: 1.77 cm^2), then 1.0 mL and 6.0 mL of phosphate-buffered saline (PBS) was applied to the SC side (donor compartment) and the dermis side (receiver compartment), respectively. The skin was hydrated for 1 h with PBS, then the applied PBS in the donor compartment was removed, and the excess water on the SC was blotted with a sheet of Kimwipe. FD-4 solution at a concentration of 10 mg/mL was prepared by completely dissolving FD-4 in PBS. The FD-4 solution (1.0 mL) was applied to the donor compartment. The permeation experiments were performed at 37°C, and the receiver solution was stirred continuously with a star-head-type magnetic stirrer. At predetermined times, an aliquot (0.5

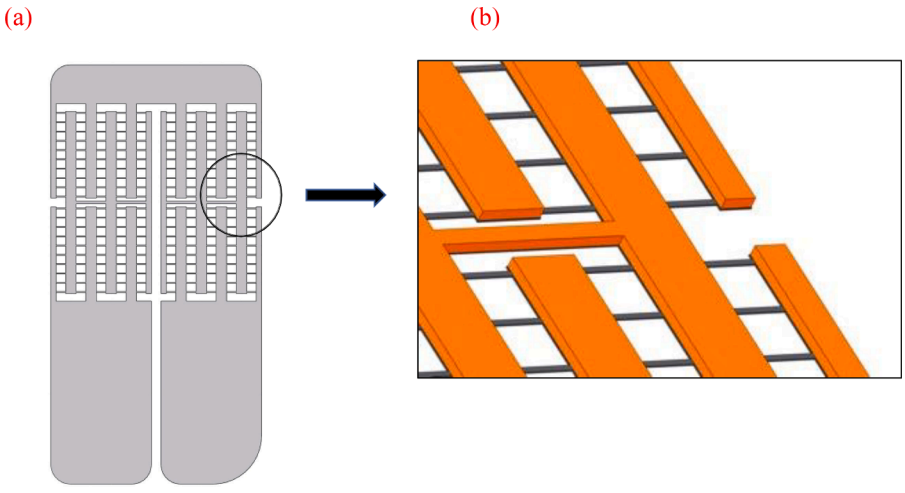

Fig. 1. Array pattern of filaments on the PassPort® system
(a) Overall array observation (200 filaments), (b) Close-up one of the filaments
The porator in PS involves 200 resistive stainless filaments distributed within $1cm^2$ and connected with thick conductive copper traces/paths. Filament are simultaneously heated for designated periods (1.1 ms, 2 ms, or 4 ms), and achieve 600°C to 700°C degrees.

mL) was withdrawn from the receiver solution and the same volume of fresh solution was added to keep the volume constant. Each experiment was performed with three to four replicates. Stripped skin was prepared by tape-stripping of the SC 30 times with adhesive tape.

The concentration of FD-4 in the receiver solution was assayed using a fluorescence spectrophotometer (RF-5300PC, Shimadzu Corporation, Kyoto, Japan) to determine the cumulative amount of FD-4 that permeated through the skin. The excitation wavelength and emission wavelength for FD-4 were 490 and 520 nm, respectively.

2.5. Calculation of skin permeation parameters

The flux and apparent permeation coefficient, P, of FD-4 were calculated from the time course profile of the cumulative amount of FD-4 that permeated through skin with the use of the following equations.

$$Flux = P \cdot C_v \tag{1}$$

where C_v is the applied concentration of FD-4. *Flux* was calculated by dividing the slope of the linear portion of the regression line with three to four successive points over 5–8 h of the application period.

2.6. Measurement of micropores created by PS treatment

After PS treatment on the dermatomed skin (thickness was set to be 550 μm), a small amount of methylene blue aq. solution was applied to the PS-treated area of skin for 5 min. After excess methylene blue solution was removed with a sheet of Kimwipe, the skin surface was observed using an optical microscope (VHX-5000, KEYENCE Corp., Osaka, Japan). The size of the pore created by PS treatment was calculated using three-dimensional shape-measurement software (VHX-H4M, KEYENCE Corp.). The depth of the pore was determined using a depth composition image, which was obtained by compiling images in different focal planes. The depth of the center of the long side of the created rectangular pore was measured. The average dimension of pores was calculated from 600 pores (three replicates).

2.7. In vivo experiment

2.7.1. Blood insulin concentration profiles

Under triple anesthesia (intraperitoneal administration of 0.15 mg/kg medetomidine hydrochloride, 2.5 mg/kg butorphanol, and 2 mg/kg midazolam tartrate), insulin solution (0.5 U/mL) was administered subcutaneously (*s.c.*; 0.25 U/kg) using a 26 G needle into the right lateral abdomen or administered transdermally (0.5 U/kg) to the PS-treated area (right lateral abdomen of male Wistar rats). The PS application site was shaved using an electric shaver 1 day before insulin application. Then, a cylindrical glass cell was attached with a glue to keep the applied insulin solution on the application site under occluded conditions with parafilm. Blood was collected from the left jugular vein over time, and the same volume of saline solution was injected into the right jugular vein. The blood was collected in a heparin-treated tube and centrifuged (15,000 rpm, 5 min) to obtain plasma. The concentration of human insulin in the plasma sample was measured using an ELISA kit (Mercodia, Uppsala, Sweden) in accordance with the manufacturer's protocol. The detection limit of the ELISA assay kit used in the study was 0.07 mU/mL.

2.8. Skin barrier recovery after PS treatment

PS treatment was done to the abdomen of hairless rats under intraperitoneal administration of triple anesthesia as above.

Skin barrier recovery after PS treatment was evaluated by measuring the change in skin impedance over 12 h. Skin impedance was measured using an impedance meter (AS-TZ1, Asahi Techno Lab, Yokohama, Japan). For the measurement of skin impedance, PBS was applied to the PS-treated area and non-PS-treated area 30 s before the measurement, then Ag and AgCl electrodes were placed on the PS-treated and non-PS-treated areas, respectively, to measure the impedance. Changes in the skin impedance were calculated using the following Eq. (2);

$$Changes\ in\ skin\ resistance\ (\%) = \frac{Skin\ resistance\ at\ time\ -\ skin\ resistance\ before\ PS-treatment}{skin\ resistance\ just\ before\ PS-treatment} \times 100 \tag{2}$$

2.9. Statistical analysis

All experiments were conducted at least in triplicates. JMP® Pro software (ver. 14.0.0, SAS Institute Inc., Cary, NC, USA) was used for statistical analyses. Experimental data were tested for statistical significance ($p < 0.05$) using one-way ANOVA and Tukey's honestly significant difference post hoc analysis. All data were expressed as the mean with standard error.

3. Theoretical

According to skin anatomy and barrier function, skin is generally divided into two or three different layers: SC, viable epidermis, and dermis. The skin permeation of drugs can be expressed using a parallel skin permeation-resistance model Wu et al., 2006). The total skin resistance (R_{tot}), where permeation resistance, R, is represented as the reciprocal of the permeability coefficient obtained from skin permeation experiments with intact skin ($1/P_{tot}$). R_{tot} is composed of resistance in the SC (R_{sc}) and the viable epidermis and dermis (R_{ved}), as shown in Eq. ((3).

$$R_{tot} = R_{sc} + R_{ved} \tag{3}$$

where R_{ved} is obtained from permeation experiments with stripped skin. R_{sc} is the difference between R_{tot} and R_{ved}. Furthermore, R_{sc} can be considered as the sum of a number (n) of the same resistance (r_{sc}) connected in parallel, as shown in Fig. 2. The R_{sc} is expressed as follows:

$$\frac{1}{R_{sc}} = \frac{1}{r_{sc}} + \frac{1}{r_{sc}} + \cdots + \frac{1}{r_{sc}} = \frac{n}{r_{sc}} \tag{4}$$

where n is number of created pores. When 200 pores were created by PS application in the SC, the skin resistance, $R_{sc}^{'}$, could be expressed as follows:

$$\frac{1}{R'_{sc}} = \frac{1}{r_{sc}} + \frac{1}{r_{sc}} + \cdots + \frac{1}{r_{sc}} + \frac{1}{r_p} + \frac{1}{r_p} + \cdots + \frac{1}{r_p} \tag{5}$$

$$= \frac{n-200}{r_{sc}} + \frac{200}{r_p} \tag{6}$$

Then, $R_{sc}^{'}$ is

$$R_{sc}^{'} = \frac{r_{sc} r_p}{(n-200) r_p + 200 r_{sc}} \tag{7}$$

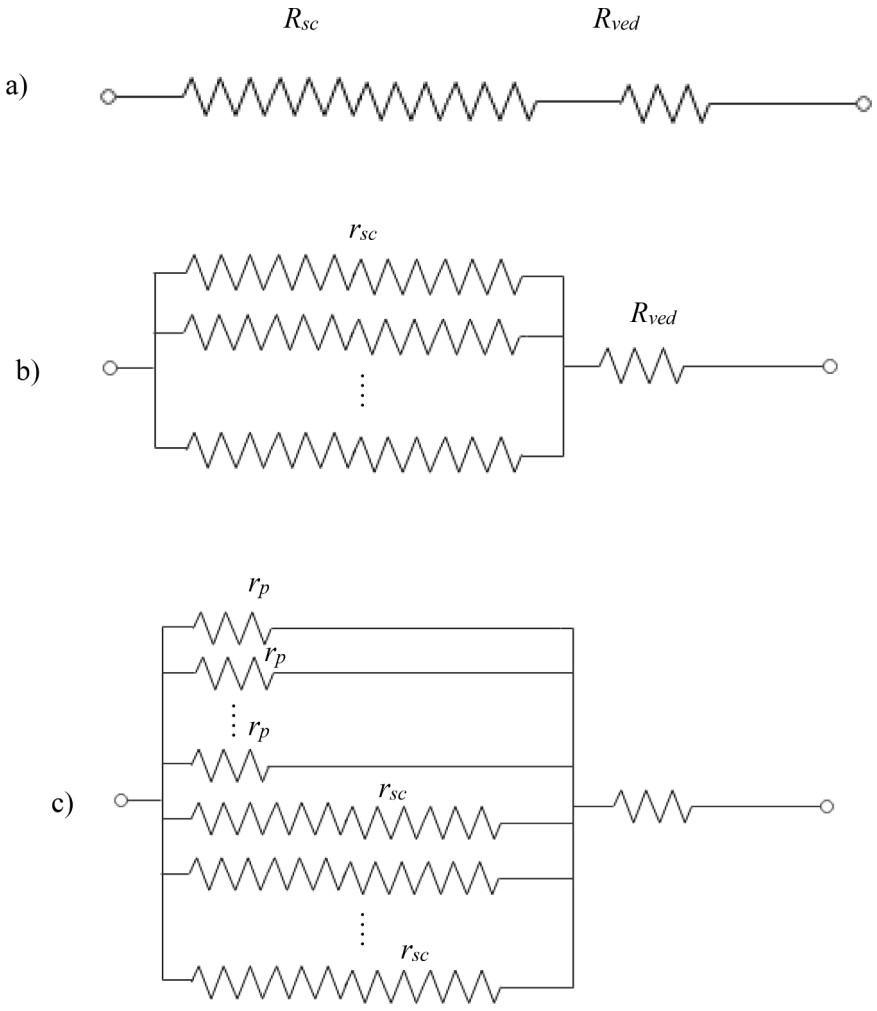

Fig. 2. Schematic representation of a skin permeation resistance model.
a: Resistance model for intact skin; b: Parallel resistance model for intact skin; c: Resistance model for punctured skin.

where r_p is the permeation resistance through one created pore.

In the present study, YMP about 20 μm thick and consisting of about 15 layers (Fujii et al., 1997) was used the *in vitro* skin permeation test. According to the depth of the micropores created after PS treatment, Eqs. 3 or 4 were applied to calculate the *P* value.

4. Results

4.1. Measurement of the size of pores in PS-treated skin

Fig. 3 shows the top view (a and b) and composite three-dimensional images (c) of PS-treated skin. Methylene blue solution was applied to the skin surface after PS treatment to observe the pores. No distinct pores were observed from a wide field microscopic view (Fig. 3a), whereas 200 pores with dimensions of about 40 μm by 320 μm were observed in the enlarged view independent of the PS treatment period. Fig. 3b shows one of the pores created by PS treatment. The three-dimensional images (Fig. 3c) were successfully composited, and the pore depth was measured from the obtained images. Fig. 3d shows measurement depth results of created pore from constructed three-dimensional images. The depth of the center of the long side of the rectangular pore (shown in a light blue color) was measured, and the obtained depth in this case was 21.44 μm.

Table 1 shows the average values obtained using the microscopy measurements. The dimensions of the observed pores from the top view were almost the same as expected from the PS treatment period. On the other hand, pore depths were 13.0, 17.7, and 21.2 μm as increasing of energy duration (1.1, 2.0, and 4 ms). Pore depths over 20 μm were observed after PS treatment. The T_{area} calculated from an area of approximately 40 μm by 320 μm was about 2.8%.

4.2. Skin permeation profile of FD-4 after PS treatment

Fig. 4 shows the results of the effect of PS treatments on the skin permeability of FD-4. Stripped skin and intact skin (with no PS treatment) were used as positive and negative controls, respectively. When FD-4 solution was applied on the stripped skin, approximately 4500-fold higher cumulative amount of FD-4 permeated over 8 h (Q_{8h}). PS treatment improved the skin permeation of FD-4, and the enhancement effects on Q_{8h} were 930-, 648-, and 474-fold for $PS_{4.0ms}$, $PS_{2.0ms}$, and $PS_{1.1ms}$, respectively.

4.3. FD-4 permeation through pores created using PS treatment

Obtained P_{tot} and P_{ved} through intact skin and stripped skin were $(2.55 \pm 0.25) \times 10^{-10}$ cm/s and $(1.15 \pm 0.11) \times 10^{-6}$ cm/s, respectively, and the calculated P_{sc} from the subtraction of $1/P_{ved}$ from $1/P_{tot}$ was 2.55×10^{-10} cm/s. On the other hand, the P_{tot} values after PSs and PSw treatments were $(2.38 \pm 0.44) \times 10^{-7}$ cm/s and $(1.47 \pm 0.17) \times 10^{-7}$ cm/s, respectively. The n calculated from the dimension of the pores created using PS treatment was 7813, and r_{sc} was determined to be 3.06×10^{13} s/cm using Eq. 3. In addition, the r_p values of the $PS_{4.0ms}$ and

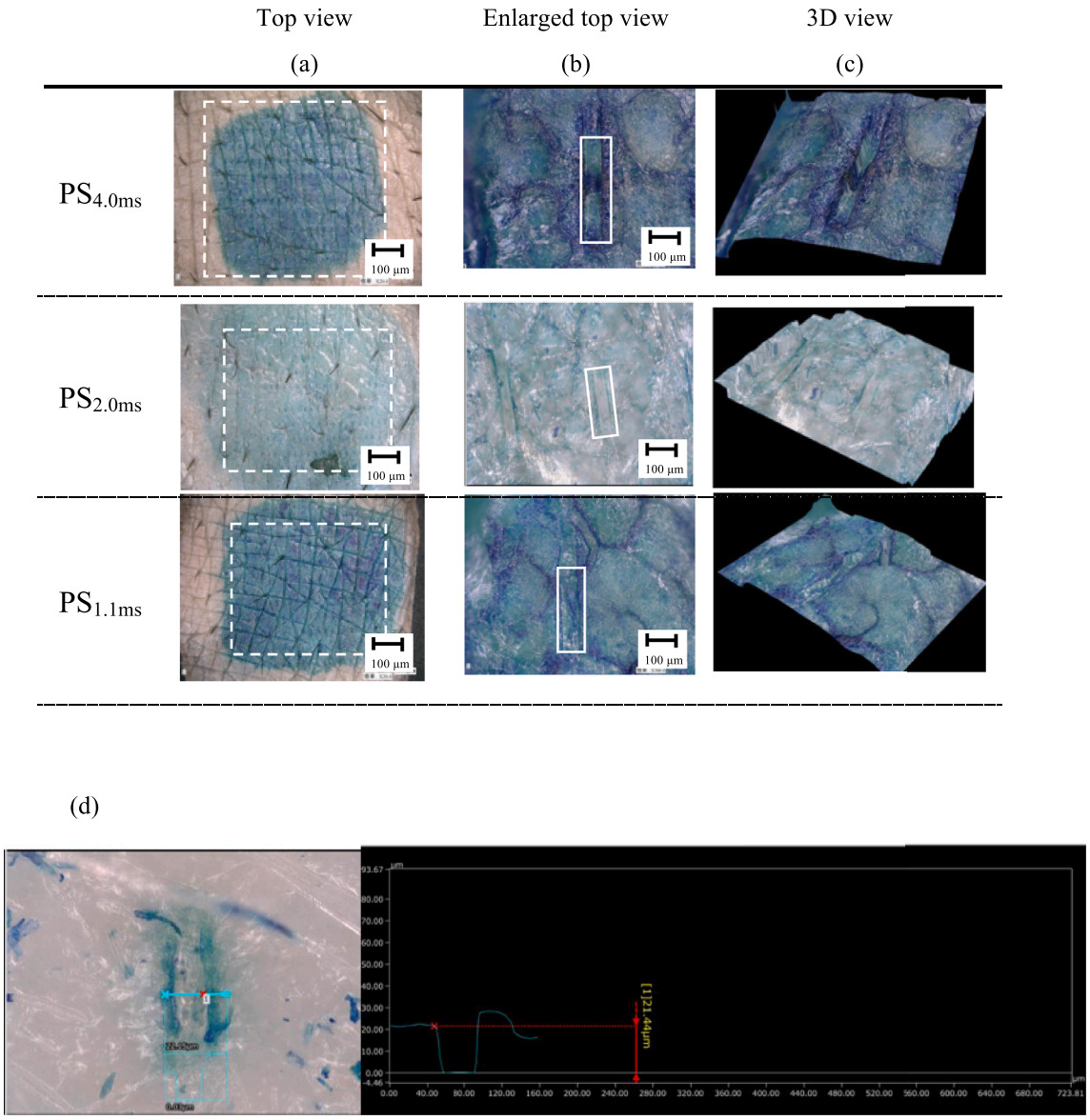

Fig. 3. 3D microscopic observation of the skin surface after PS application. Treatment of the skin with methylene blue aqueous solution was conducted to observe the pores created. Dotted line: PS application area, solid line; created micropore. (a) top view, (b) enlarged top view, (c) 3D view, (d) Measurement depth results of the created pores (right part) from the constructed three-dimensional image (left part) (The arrow shows the measurement part) (For interpretation of the references to color in this figure legend, the reader is referred to the web version of this article.).

Table 1
Measurement of the size of pores created by thermalporation.

	Average ± S.D. (μm)		
Treatment	Length	Width	Depth
$PS_{4.0ms}$	321.3 ± 1.7	42.1 ± 1.4	21.2 ± 5.9
$PS_{2.0ms}$	322.4 ± 1.4	40.7 ± 1.4	17.7 ± 4.2
$PS_{1.1ms}$	326.8 ± 2.2	41.9 ± 5.4	13.0 ± 2.2

$PS_{1.1ms}$ treatments were 6.67×10^8 s/cm and 1.19×10^9 s/cm, respectively.

4.4. Blood glucose and insulin profiles after transdermal administration of insulin through PS-treated skin

Fig. 5 shows the blood concentration profile of insulin after *s.c.* injection as well as the transdermal application after $PS_{4.0ms}$ treatment. Only $PS_{4.0ms}$ was applied in the present study because it showed the highest skin permeation effect for FD-4, and two-fold higher insulin dose was applied for transdermal application in order to obtain quantitative blood concentrations of insulin. Rapidly increased blood concentrations of insulin were observed after *s.c.* injection, and the concentrations decreased after reaching the maximum concentration (C_{max}) approximately 30 min after administration. The insulin concentration reached a level lower than the minimum detectable concentration (3.3 μU/mL) at 360 min after administration. On the other hand, PSs application provided a gradual increase in the blood concentration of insulin. The concentration reached C_{max} after approximately 360 min and was still detectable until 720 min after application. The areas under the blood concentration–time curve up to 12 h after administration (AUC_{12h}) (calculated using the trapezoidal equation) were 3345 and 1413 μU«min/mL for *s.c.* injection and transdermal application with $PS_{4.0ms}$, respectively. The relative bioavailability was 21.1% after transdermal application of insulin with $PS_{4.0ms}$.

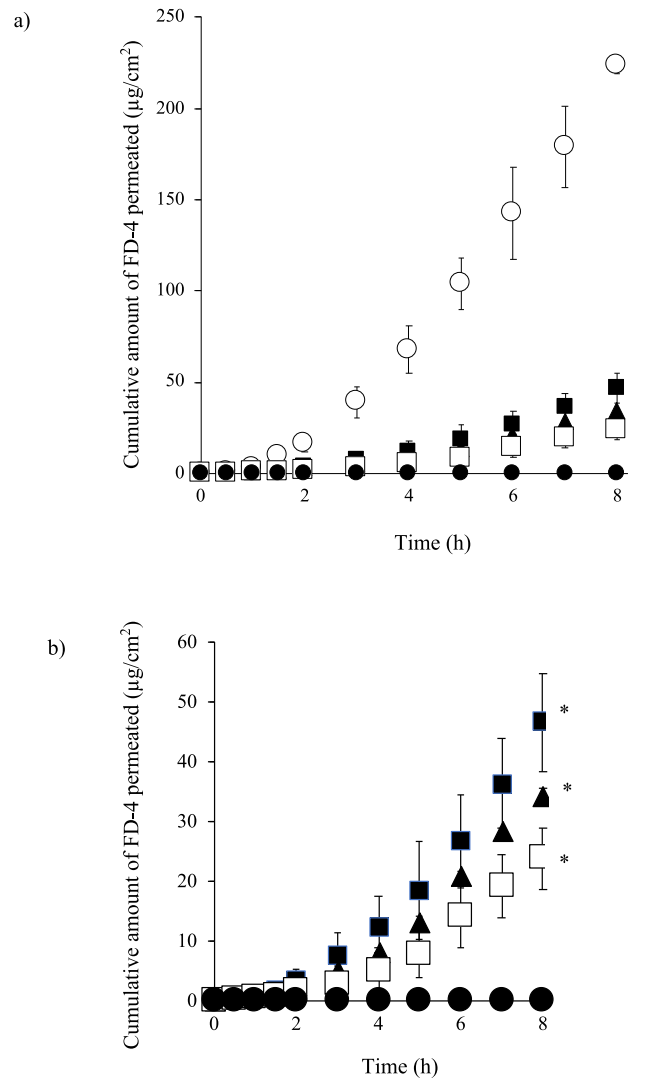

Fig. 4. Cumulative amount of FD-4 permeated through hairless rat skin. Symbols: ●; intact skin (without PS application) ○; stripped skin, □; $PS_{1.1ms}$ applied intact skin, ▲; $PS_{2.0ms}$ applied intact skin, ■; $PS_{4.0ms}$ applied intact skin. Each point shows the mean ± S.E. (n = 3–4). $P<0.05$ compared with Q_{8h} of intact skin.

4.5. Barrier recovery of PS-treated skin

Change in the barrier function of the SC was investigated with the change in the skin resistance value to evaluate barrier function recovery after PS treatments (Fig. 6). Skin resistance value decreased dramatically just after PS treatments and about 90% of decreased skin resistance was obtained irrespective of the type of PS treatment. Then, the resistance value gradually returned to the initial skin resistance value over 12 h, independent of the created pore depth.

5. Discussion

$PS_{4.0ms}$ treatment exhibited approximately 930-fold higher skin permeation of FD-4 than that without PS treatment. A skin permeation resistance model shown in Fig. 2 was used for analysis of the enhancement effect by PS treatment. The r_p values calculated with permeation profiles through $PS_{4.0ms}$- and $PS_{1.1ms}$-treated skin were 6.67×10^8 and 1.19×10^9 s/cm, respectively. The ratio of $1/r_p$ obtained from $PS_{1.1ms}$ treatment against that from $PS_{4.0ms}$ treatment was 0.56. This value was almost same as the ratio of the depth of pores created using $PS_{1.1ms}$ versus those using $PS_{4.0ms}$ (0.61). This result suggested that FD-4 permeation through PS-treated skin was dependent on the depth of pores created in the SC. In addition, R'_{sc} values may be changed by the pore size (height and width) and the number of pores. The present resistance model may be useful to estimate the skin permeation of drugs even when the number and size of stainless filaments in the PS device was changed. FD-4 is more stable in the skin compared with insulin. Thus, FD-4 was selected as a model drug, and estimation of insulin absorption was done using the FD-4 permeation date, which has almost the same molecular size as insulin.

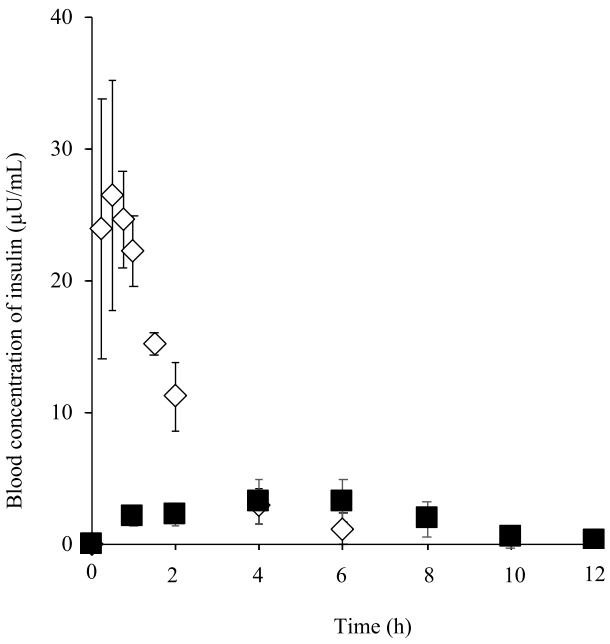

Fig. 5. Blood insulin concentration–time profiles
Symbols; ⋄; *s.c.* injection, ■; transdermal application after PSs treatment. Each point shows the mean ± S.E. (n = 3–4).

Topically applied insulin after $PS_{4.0ms}$-treatment was absorbed into the systemic circulation via blood capillaries in the epidermis. Needle-free injections and hollow microneedles can directly deliver drugs into the epidermis and dermis, and rapid drug absorption may be obtained by drug administration with these devices (Harvey et al., 2011; Inoue et al., 2010). On the other hand, PS treatment provided gradually increased insulin concentrations in the blood, as shown in Fig. 5, because it took time for the insulin to reach capillaries in the epidermis through the viable epidermis. The drug absorption rate may be influenced by the vicinity of the dermal vasculature. A tight junction barrier is located in the granular layer of the epidermis (Pummi et al., 2001). Thus, application of tight junction modulators such as sodium caprate and AT1002 might be effective in increasing the skin permeation rate of a middle molecular weight biomedical agents (Gopalakrishnan et al., 2009; Kurasawa et al., 2009). When blood insulin concentration was compared between *s.c.* injection and $PS_{4.0ms}$ treatment, $PS_{4.0ms}$ treatment provided a gradual increase in insulin concentration and maintained a constant concentration. This obtained profile seemed to exhibit the characteristics of drug delivery with PS treatment very well. In other words, PS treatment may be suitable as a drug administration device that does not require rapid blood migration after application.

Assuming that insulin permeates through $PS_{4.0ms}$-treated skin with a P value of 2.38×10^{-7} cm/s with a 2 h lag-time, which was obtained from FD-4 permeation experiments, the amount of permeated insulin was about 9×10^{-3} U at 8 h after application. If the permeated insulin had migrated completely into the systemic circulation, about 9.0% of the applied insulin was absorbed in the present experimental conditions. However, the bioavailability obtained from *in vivo* experiments was 21.1%. The absorption ratio calculated from the *in vitro* experiment with

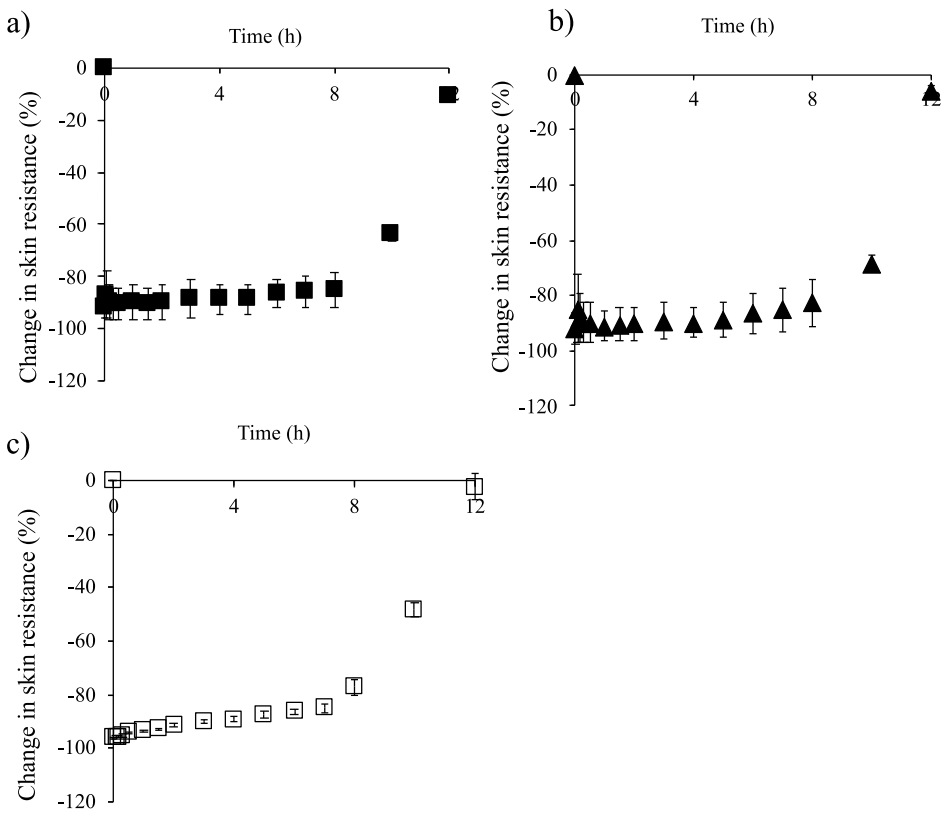

Fig. 6. Change in skin resistance value
(a) ■; $PS_{4.0ms}$ applied intact skin, (b) ▲; $PS_{2.0ms}$ applied intact skin, (c) □; $PS_{1.1ms}$ applied intact skin. Dotted lines show the skin resistance value before PS application. Each point shows the mean ± S.E. (n = 3–4).

YMP skin was about 0.43-fold underestimated from *in vivo* experiment results with rats, suggesting that differences between species in skin permeation between rat and porcine models might have affected the results. However, the skin resistance model obtained from *in vitro* experiment can be utilized to roughly estimate *in vivo* absorption ratio.

Unlike the above problem, the applied insulin solution tended to gather in the peripheral area of the glass cell easily over time because the abdomen at the application site was not horizontal. This phenomenon might affect the blood concentration–time profile of insulin. Formulation to hold applied solution on the PS treated site and a combination of other driving forces, such as electroosmosis generated by iontophoresis, is necessary to increase utilization of the applied drug after PS application.

The barrier function of the SC had almost recovered by 12 h after PS treatment. Kam et al. reported barrier recovery evaluated in guinea pigs, and the transepidermal water loss (TEWL) value recovered 24 h after radiofrequency microchannel treatment, which is a thermal abrasion technique (Kam et al., 2012). Lee et al. also evaluated the change in barrier function recovery with TEWL. They reported that pores created by laser abrasion with microchannels of about 150 μm in diameter and 25 μm in depth were restored at 16 h after irradiation (Lee et al., 2003). In addition to thermal ablation, TEWL recovery within 24 h after the application of physical means to produce microchannels in the SC, such as microneedle treatments (Haq et al., 2009), and electroporation (Sugibayashi et al., 2010), has also been reported. In the present study, skin resistance almost recovered to the initial level by 12 h. In addition, TEWL values after the application of PS treatment returned to the level before PS treatment after 12 h (Supplemental Fig. S1). Furthermore, micropores created after the application of $PS_{4.0ms}$ treatment was closed gradually, with the passage of time, although it was a visible observation (Supplemental Fig. S2).

From a safety perspective, a rapid recovery after PS treatment will be preferable. However, a slow recovery might be preferable in order to obtain skin permeation enhancement effects after PS treatment because a quick recovery may decrease the skin permeation of a drug. Tokudome et al. reported that delays in repair of the SC after treatment using electroporation provided a higher skin permeation of macromolecules (Tokudome and Sugibayashi, 2003). Thus, from the point of view of enhancement of skin permeation, the lifetime of the created pore route will be important in governing drug transport. A hydration process may prolong the recovery period of the abraded SC, and negatively charged materials on the skin might accelerate repair of the barrier function of the SC. Currently, there are no criteria for the repair of barrier function after skin abrasion, which has the skin permeation enhancement effect and enables safe use. However, control of repair of the skin barrier will be an important point for practical use of thermal ablation as well as other physical means. In the present study, recovery of the skin barrier was investigated; however, measurement of the recovery of skin resistance does not evaluate pathological damage to the skin by PS treatment. Further studies with histological observations should be done to evaluate the safety of PS treatment.

In addition to PS treatment, other physical devices such as solid type microneedles and electroporation can also create micropores in the SC. Understanding the differences in the characteristics of skin permeation among these devices will help in the selection of devices that allow increased permeation of specific drugs depending on the therapeutic purpose. PS treatment applies from the surface of skin, and then the transdermal patch is covered on the microporated skin. Unlike with microneedles, PS treatment may be safer and have advantages due to needle-free injection. In the present study, *in vivo* experiments were done with insulin only. Other middle molecular weight drugs should be applied to confirm the features of the blood concentration–time profiles after PS treatment. Furthermore, a resistance model should be applied with different filament sizes and arrangements. Further experiments are

needed to clarify the differences in efficacy and safety.

5. Conclusion

Pores created by thermalporation were effective in improving the skin permeation of FD-4 and insulin. In the present study, it was not examined whether PS treatment caused skin irritation or lipohypertrophy, which are known to be caused by repeated *s.c.* injection (Gentile et al., 2016). Although further study on the safety of the application of the device should be considered, PS treatment was associated with the maintenance of blood concentrations of drugs for a long period, although their absorption rate was slow. Therefore, considering the characteristics of drug absorption through PS-treated skin, PS treatment was considered to be suitable for the transdermal application of hormones and central nervous system drugs.

CRediT authorship contribution statement

Naoto Ono: Methodology, Formal analysis, Investigation. **Tomoya Iibuchi:** Methodology, Formal analysis, Investigation. **Hiroaki Todo:** Supervision, Writing – original draft. **Shoko Itakura:** Data curation. **Hirotoshi Adachi:** Resources. **Kenji Sugibayashi:** Project administration, Writing – review & editing.

Declaration of Competing Interest

The authors declare no conflict interest associated with this manuscript.

Supplementary materials

Supplementary material associated with this article can be found, in the online version, at doi:10.1016/j.ejps.2021.106096.

References

Badkar, A.V., Smith, A.M., Eppstein, J.A., Banga, A.K., 2007. Transdermal delivery of interferon Alpha-2B using microporation and iontophoresis in hairless rats. Pharm. Res. 24, 1389–1395. https://doi.org/10.1007/s11095-007-9308-2.

Bramson, J., Dayball, K., Evelegh, C., Wan, Y.H., Page, D., Smith, A., 2003. Enabling topical immunization via microporation: A novel method for pain-free and needle-free delivery of adenovirus-based vaccines. Gene Ther. https://doi.org/10.1038/sj.gt.3301886.

Fujii, M., Yamanouchi, S., Hori, N., Iwanaga, N., Kawaguchi, N., Matsumoto, M., 1997. Evaluation of Yucatan micropig skin for use as an in vitro model for skin permeation study. Biol. Pharm. Bull. 20, 249–254. https://doi.org/10.1248/bpb.20.249.

Gentile, S., Strollo, F., Ceriello, A., 2016. Lipodystrophy in insulin-treated subjects and other injection-site skin reactions: are we sure everything is clear? Diabetes Ther. 7, 401–409. 10.1007/s13300-016-0187-6.

Gopalakrishnan, S., Pandey, N., Tamiz, A.P., Vere, J., Carrasco, R., Somerville, R., Tripathi, A., Ginski, M., Paterson, B.M., Alkan, S.S., 2009. Mechanism of action of ZOT-derived peptide AT-1002, a tight junction regulator and absorption enhancer. Int. J. Pharm. 365, 121–130. https://doi.org/10.1016/j.ijpharm.2008.08.047.

Haq, M.I., Smith, E., John, D.N., Kalavala, M., Edwards, C., Anstey, A., Morrissey, A., Birchall, J.C., 2009. Clinical administration of microneedles: skin puncture, pain and sensation. Biomed. Microdevices 11, 35–47. https://doi.org/10.1007/s10544-008-9208-1.

Harvey, A.J., Kaestner, S.A., Sutter, D.E., Harvey, N.G., Mikszta, J.A., Pettis, R.J., 2011. Microneedle-based intradermal delivery enables rapid lymphatic uptake and distribution of protein drugs. Pharm. Res. 28, 107–116. https://doi.org/10.1007/s11095-010-0123-9.

Hogan, N.C., Taberner, A.J., Jones, L.A., Hunter, I.W., 2015. Needle-free delivery of macromolecules through the skin using controllable jet injectors. Expert Opin. Drug Deliv. 12, 1637–1648. https://doi.org/10.1517/17425247.2015.1049531.

Inoue, N., Todo, H., Iidaka, D., Tokudome, Y., Hashimoto, F., Kishino, T., Sugibayashi, K., 2010. Possibility and effectiveness of drug delivery to skin by needle-free injector. Int. J. Pharm. 391, 65–72. https://doi.org/10.1016/j.ijpharm.2010.02.019.

Kam, Y., Sacks, H., Kaplan, K.M., Stern, M., Levin, G., 2012. Radio frequency-microchannels for transdermal delivery: characterization of skin recovery and delivery window. Pharmacol. Pharm. 03, 20–28. https://doi.org/10.4236/pp.2012.31004.

Kurasawa, M., Kuroda, S., Kida, N., Murata, M., Oba, A., Yamamoto, T., Sasaki, H., 2009. Regulation of tight junction permeability by sodium caprate in human keratinocytes and reconstructed epidermis. Biochem. Biophys. Res. Commun. 381, 171–175. https://doi.org/10.1016/j.bbrc.2009.02.005.

Lee, W.R., Shen, S.C., Wang, K.H., Hu, C.H., Fang, J.Y., 2003. Lasers and microdermabrasion enhance and control topical delivery of Vitamin C. J. Invest. Dermatol. 121, 1118–1125. https://doi.org/10.1046/j.1523-1747.2003.12537.x.

Nagamune, T., 2017. Biomolecular engineering for nanobio/bionanotechnology. Nano Converg. 4 (9) https://doi.org/10.1186/s40580-017-0103-4.

Park, J.H., Lee, J.W., Kim, Y.C., Prausnitz, M.R., 2008. The effect of heat on skin permeability. Int. J. Pharm. 359, 94–103. https://doi.org/10.1016/j.ijpharm.2008.03.032.

Prausnitz, M.R., 2004. Microneedles for transdermal drug delivery. Adv. Drug Deliv. Rev. 56, 581–587. https://doi.org/10.1016/j.addr.2003.10.023.

Prausnitz, M.R., Langer, R., 2008. Transdermal drug delivery. Nat. Biotechnol. 26, 1261–1268.

Pummi, K., Malminen, M., Aho, H., Karvonen, S.L., Peltonen, J., Peltonen, S., 2001. Epidermal tight junctions: ZO-1 and occludin are expressed in mature, developing, and affected skin and *in vitro* differentiating keratinocytes. J. Invest. Dermatol. 117, 1050–1058. https://doi.org/10.1046/j.0022-202X.2001.01493.x.

Sawyer, J., Febbraro, S., Masud, S., Ashburn, M.A., Campbell, J.C., 2009. Heated lidocaine/tetracaine patch (Synera™, Rapydan™) compared with lidocaine/prilocaine cream (EMLA®) for topical anaesthesia before vascular access. Br. J. Anaesth. 102, 210–215. https://doi.org/10.1093/bja/aen364.

Sintov, A.C., Krymberk, I., Daniel, D., Hannan, T., Sohn, Z., Levin, G., 2003. Radiofrequency-driven skin microchanneling as a new way for electrically assisted transdermal delivery of hydrophilic drugs. J. Control. Release 89, 311–320. https://doi.org/10.1016/S0168-3659(03)00123-8.

Sugibayashi, K., Todo, H., Yamaguchi, K., 2010. Effect of negative charged particles on the recovery of skin barrier function after EP treatment. J. Drug Deliv. Sci. Technol. 20, 445–450. https://doi.org/10.1016/S1773-2247(10)50077-7.

Sulaiman, Al D, Chang, J.Y.H., Bennett, N.R., Topouzi, H., Higgins, C.A., Irvine, D.J., Ladame, S., 2019. Hydrogel-coated microneedle arrays for minimally invasive sampling and sensing of specific circulating nucleic acids from skin interstitial fluid. ACS Nano 13, 9620–9628. https://doi.org/10.1021/acsnano.9b04783.

Tokudome, Y., Sugibayashi, K., 2003. The effects of calcium chloride and sodium chloride on the electroporation-mediated skin permeation of fluorescein isothiocyanate (FITC)-dextrans *in vitro*. Biol. Pharm. Bull. 26, 1508–1510. https://doi.org/10.1248/bpb.26.1508.

Waghule, T., Singhvi, G., Dubey, S.K., Pandey, M.M., Gupta, G., Singh, M., Dua, K., 2019. Microneedles: a smart approach and increasing potential for transdermal drug delivery system. Biomed. Pharmacother. 109, 1249–1258. https://doi.org/10.1016/j.biopha.2018.10.078.

Wood, D.G., Brown, M.B., Jones, S.A., 2011. Controlling barrier penetration via exothermic iron oxidation. Int. J. Pharm. 404, 42–48. https://doi.org/10.1016/j.ijpharm.2010.10.047.

Wu, X.M., Todo, H., Sugibayashi, K., 2006. Effects of pretreatment of needle puncture and sandpaper abrasion on the in vitro skin permeation of fluorescein isothiocyanate (FITC)-dextran. Int. J. Pharm. 316, 102–108. https://doi.org/10.1016/j.ijpharm.2006.02.046.

Zhao, Y., Murthy, S., Manjili, M., Guan, L., Sen, A., Hui, S., 2006. Induction of cytotoxic T-lymphocytes by electroporation-enhanced needle-free skin immunization. Vaccine 24, 1282–1290. https://doi.org/10.1016/j.vaccine.2005.09.035.